[15]Schooley, A. H., "Wake Collapse in a Stratified Fluid: Experimental Exploration of Scaling Characteristics," *Science*, Vol. 160, 1968, pp. 763–764.

[16]Wu, J., "Mixed Region Collapse with Internal Wave Generation in a Density Stratified Medium," *Journal of Fluid Mechanics*, Vol. 35, 1969, pp. 531–544.

[17]Smith, T. B. and Diamond, R. J., "Studies of Contrails from Jet Powered Aircraft," Final Rept. Contract AF19(604)-1495, 1955, Meteorology Research, Inc., Pasadena, Calif.

[18]Smith, T. B. and Beesmer, K. M., "Contrail Studies for Jet Aircraft," Final Report Contract AF19(604)-2038, 1959, Meteorology Research, Inc., Pasadena, Calif.

[19]Overcamp, T. J., "Dispersion of the Exhaust of a Supersonic Transport in the Stratosphere," Ph.D. thesis, Massachusetts Institute of Technology, Dept. of Mechanical Engineering, Cambridge, Mass., Feb. 1973.

[20]Landahl, M. T. and Widnall, S. E., "Vortex Control," *Aircraft Wake Turbulence and Its Detection*, edited by J. H. Olsen, A. Goldburg, and M. Rogers, Plenum Press, New York, 1971, pp. 137–155.

[21]Olsen, J. H., "Results of Trailing Vortices in a Towing Tank," *Aircraft Wake Turbulence and Its Detection*, edited by J. H. Olsen, A. Goldburg, and M. Rogers, Plenum Press, New York, 1971, pp. 455–472.

[22]Bilanin, A. J. and Widnall, S. E., "Aircraft Wake Dissipation by Sinusoidal Instability and Vortex Breakdown," AIAA Paper No. 73-107, Washington, D.C., 1973.

[23]Hoult, D. P. and Weil, J. C., "Turbulent Plume in a Laminar Cross Flow," *Atmospheric Environment*, Vol. 6, 1972, pp. 513–532.

[24]Tsang, G., "Laboratory Study of Line Thermals," *Atmospheric Environment*, Vol. 5, 1971, pp. 445–471.

[25]Dopplick, T. G., "Global Radiative Heating of the Earth's Atmosphere," Planetary Circulation Project Rept. 24, 1970, Department of Meteorology, MIT, Cambridge, Mass.

[26]Rodgers, C. D. and Walshaw, C. D., "The Computation of Infrared Cooling Rate in Planetary Atmospheres," *Quarterly Journal of the Royal Meteorological Society*, Vol. 92, 1966, pp. 67–92.

[27]Yamamoto, G., "Direct Absorption of Solar Radiation by Water Vapor, Carbon Dioxide, and Molecular Oxygen," *Journal of the Atmospheric Sciences*, Vol. 19, 1962, pp. 182–190.

[28]*U.S. Standard Atmosphere Supplements, 1966*, U.S. Government Printing Office, Washington, D.C., 1966, Part 5.

[29]Sutton, O. G., *Micrometeorology*, McGraw-Hill, New York, 1953, pp. 319–322.

[30]Gudiksen, P. A., Fairhall, A. W., and Reed, R. J., "Roles of Meridinal Circulation and Eddy Diffusion in the Transport of Trace Substances in the Lower Stratosphere," *Journal of Geophysical Research*, Vol. 73, 1968, pp. 4461–4473.

Flutter of Pairs of Aerodynamically Interfering Delta Wings

Richard R. Chipman,* Frank J. Raucht†

Grumman Aerospace Corporation, Bethpage, N.Y.

AND

Robert W. Hess‡

NASA Langley Research Center, Hampton, Va.

To examine the effect on flutter of the aerodynamic interference between pairs of closely spaced delta wings, several structurally uncoupled 1/80 th-scale models were studied by experiment and analysis. Flutter test boundaries obtained in NASA Langley's 26-in. transonic blowdown wind tunnel were compared with subsonic analytical results generated using the doublet lattice method. Trends for several combinations of vertical and longitudinal wing separation were determined, showing flutter speed significantly affected in the closely spaced configurations. For some configurations, a flutter mechanism coupling flexible modes of both surfaces at a disinctive flutter frequency was predicted and observed. The flexibilities of both surfaces were concluded to be essential to the analysis.

Nomenclature

b_r	= reference semi-chord of trailing wing
c	= mean aerodynamic chord of leading wing
f	= frequency, Hz
g	= damping
h	= biplanar (vertical) wing separation
k	= stiffness matrix
l	= streamwise (longitudinal) wing separation
m	= mass matrix
M	= Mach number
q	= displacement vector of the degrees of freedom
Q	= aerodynamic force vector
V_f	= flutter velocity
$V_f(\infty)$	= V_f of flutter-critical isolated wing
$V_f(h,l)$	= V_f of a configuration with biplanar and streamwise separations, h and l
μ	= mass density ratio
ω_f	= flutter frequency, rad./sec.
ω_r	= reference frequency

Introduction

THE aerodynamic interaction of lifting surfaces in proximity can create aerodynamic forces sufficient to destabilize surfaces otherwise flutter-free within their flight envelope. This problem on various aircraft designs has stimulated the efforts of several investigators: T-tail flutter was found to be a problem by Stahle.[1] To predict unsteady aerodynamic loads on a T-tail, Stark[2] subsequently developed a subsonic nonplanar doublet-lattice theory. Similarly, Laschka[3] extended the so called kernal function method to multiple coplanar surfaces. Experiments re-

Table 1 Wing Designs

TYPE	TRAILING	LEADING	LEADING
CROSS-SECTION			
DESIGNATION	100	070/040	070/032
CORE (IN.)	0.100	0.070	0.070
ROOT CHORD (IN.)	13.5	9.0	9.0
TIP CHORD (IN.)	2.50	1.66	1.66
M.A.C. (IN.)	9.27	6.18	6.18
HINGE (IN.)	–	0.040	0.032
f_1 (Hz)	104.	129.8	129.5
f_2 (Hz)	223.	283.8	261.4

Fig. 1   Core of leading delta wing.

ported by Topp et al.[4] showed a dramatic degradation in the flutter speed of a variable sweep aircraft, due to aerodynamic and structural coupling of the wing, tail, and fuselage. Only by accounting for aerodynamic interference between the wing and tail, could this trend be calculated.[5] Exploring this phenomenon in depth, Mykytow et al.[6] conducted flutter tests on a wing-fuselage-tail model and correlated findings with predictions made using both doublet-lattic and kernel function methods developed by Albano and Rodden.[7,8] Using structurally coupled modes in the analysis of a similar configuration, Triplett et al.[9] showed that the flutter mechanism could go entirely undetected if aerodynamic forces were calculated on both the wing and tail without including their aerodynamic interference.

More recently the problem of interference flutter was of concern on flyback booster space shuttle configurations. Wind tunnel tests conducted by NASA Langley Research Center on pairs of equally sized low-sweep wings indicated that close proximity could severely affect the flutter boundary.[10]

To determine the effect of close spacing on unequally sized, highly swept delta wings, a joint analytical and experimental study was performed on pairs of 1/80th-scale shuttle wings. Specifically, various model deltas were designed, fabricated, and analyzed, and were tested at the Langley Research Center's 26-in. Transonic Blowdown Wind Tunnel. For various horizontal and vertical separations of the leading and trailing wings, test flutter boundaries were determined for the Mach number range 0.6 to 1.4. These were compared subsonically with trends derived from the application of the doublet lattice method,[11] which had been used successfully to predict interference flutter on the aforementioned low-sweep wings.[12] The results of this test program and the comparison with theory are the basis of this paper.

Test Apparatus

Models

The basic design for both the leading (orbiter) and the trailing (booster) wings was a cropped delta with a 59° L.E. sweep and an aspect ratio of 0.794. The trailing wing had a fifty % greater length and span than the leading wing. As shown in Fig. 1, each model consisted of a homogeneous aluminum alloy core plate with cut-outs designed to provide a realistic torsion-to-bending frequency ratio. The core plates had a constant thickness of 0.070 in. and
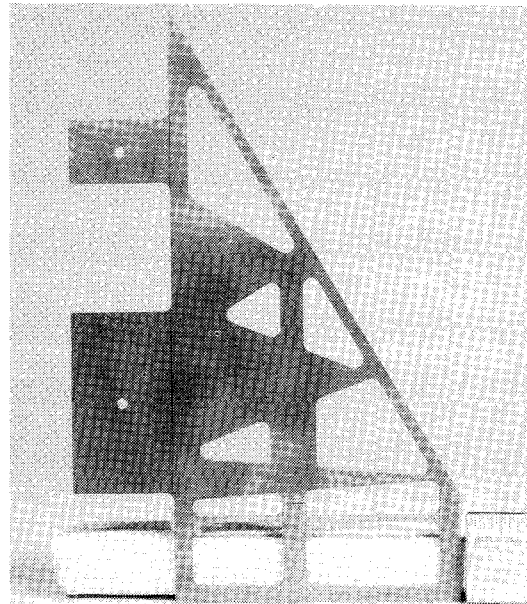
0.100 in. for the leading and trailing wing, respectively. An 8% airfoil profile was obtained by bonding to each core end-grain balsa wood with a thin mylar covering. The leading wing was equipped with a full-span control surface with sets of interchangeable hinges of various stiffnesses made of thin strips of beryllium copper. A section of the wing is shown in Fig. 2. By a simple change of hinges, the control surface could alternately be set at one of two selected stiffnesses: With the first (stiff) set, the leading wing would have a flutter boundary higher in dynamic pressure than that of the isolated trailing wing. With the second (flexible) set, the boundary would be about the same as that of the trailing wing. Table 1 summarizes the design of the three surfaces tested and lists the measured first two natural frequencies of each.

To achieve variations in the streamwise and vertical wing separations without introducing structural coupling, a rigid mounting block with various slots was made. The tangs of the wings were clamped into the desired slots and the entire assembly was bolted to a holding block and its affixed splitter plate, which were fastened to the wing tunnel wall. A typical installation is shown in Fig. 3.

Instrumentation

Each model was instrumented with strain gages which through their response to bending and torsional motions, were used to detect the onset of flutter and to measure flutter frequency. Models with control surfaces were additionally equipped with a solenoid having its coil and core plug on opposite sides of the hinge line.
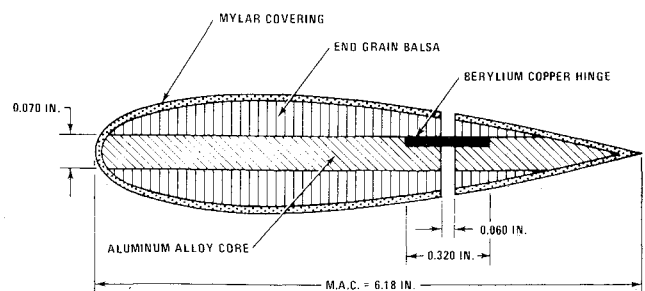

Fig. 2   Section of leading wing showing control surface detail (not to scale).
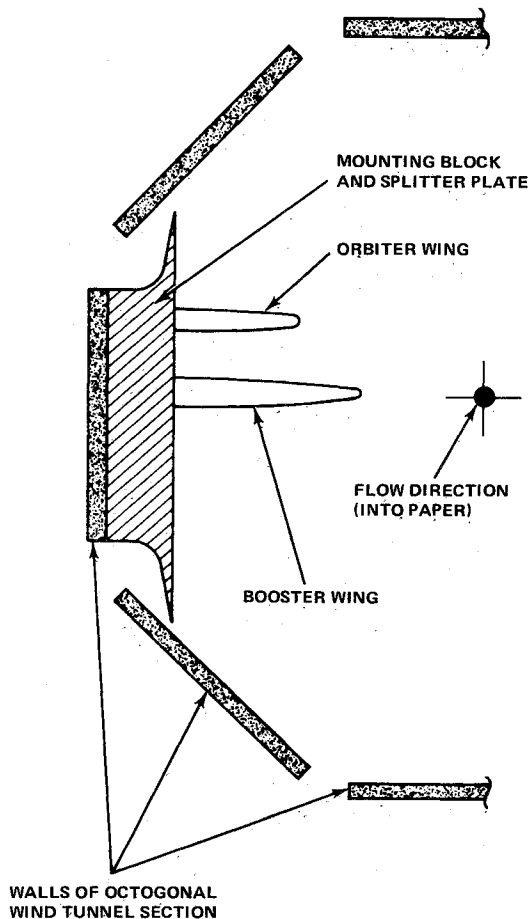
Fig. 3 Test wings in tunnel.

Wind Tunnel

Flutter tests were conducted in the NASA Langley Research Center 26-inch Transonic Blowdown Wind tunnel for a Mach number range of 0.6 to 1.4.

Test Procedure

Vibration Survey

Prior to wind tunnel testing, each model was subjected to a vibration survey. Modal shapes, frequencies and damping coefficients were determined for one model of each of the three types. Subsequent models of each type were checked for likeness of frequencies and damping coefficients. Noncontacting excitation and measurement
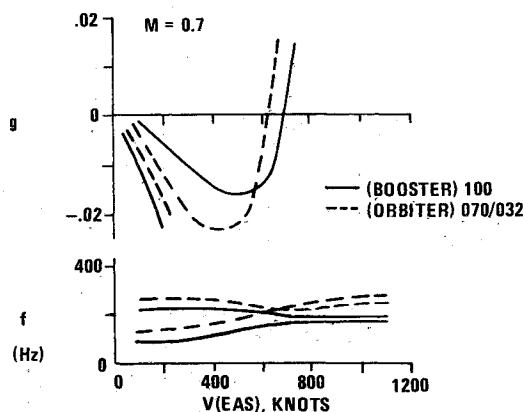

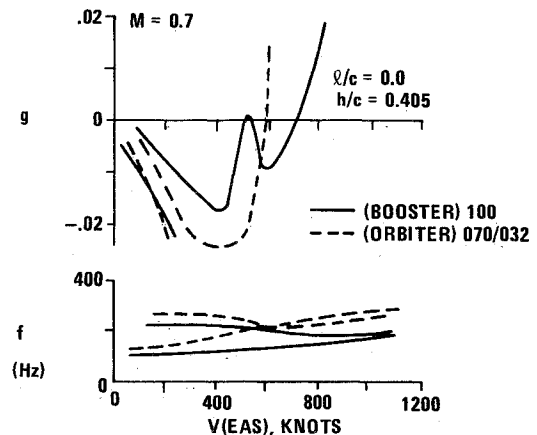Fig. 4 Flutter analysis of delta wings without aerodynamic coupling.

Fig. 5 Flutter analysis of closely spaced delta wings including aerodynamic coupling.

systems were utilized to assure distortion-free mode shapes and frequencies. The output of the noncontacting inductance-type pickup was conditioned, and displayed on a vacuum tube voltmeter and oscillograph to extract mode shapes and damping data. During the survey, the models were clamped in the mounting block that would be used in the wind tunnel so that root conditions would be the same in the tunnel installation.

Flutter Tests

Before each tunnel run, the models to be used were visually examined for signs of damage due to previous runs. In addition, after being installed in the tunnel, each model was excited, and oscillograph records of the strain gage outputs were monitored to check frequencies and dampings of the first four modes.

On the basis of the results of previous runs, a desired tunnel operating "path" was selected for the run. This path was followed until either the tunnel air supply was exhausted or flutter was detected visually. High speed films were taken during the runs to record any dynamic instability encountered. Several runs following different paths were made on each configuration to determine a boundary of flutter speed vs Mach number.

Flutter boundaries were obtained for the pairing of each of the two leading wings with the trailing wing at the various horizontal and vertical separations shown in Table 2. Additionally, boundaries for each of the three isolated wings were obtained.

Analysis

Since the present study is restricted to the effects of aerodynamic coupling, the equations of motion for a two-component system may be written

$$
\begin{bmatrix} m_{AA} & 0 \\ 0 & m_{BB} \end{bmatrix} \begin{Bmatrix} \ddot{q}_A \\ \ddot{q}_B \end{Bmatrix} + \begin{bmatrix} k_{AA} & 0 \\ 0 & k_{BB} \end{bmatrix} \begin{Bmatrix} q_A \\ q_B \end{Bmatrix} = \begin{bmatrix} Q_{AA} + Q_{AB} \\ Q_{BA} + Q_{BB} \end{bmatrix}
$$

The aerodynamic forces, including the coupling forces, Q_{AB} and Q_{BA}, are calculated for subsonic Mach numbers through use of the doublet lattice method.[11] Using measured normal modes and frequencies, flutter solutions are determined by the classical V-g method.[13] The flutter speeds and frequencies are chosen based on measured structural damping.

Representative V-g and V-f plots are shown in Figs. 4 and 5 for one of the tested configurations at a Mach number of 0.7 with and without aerodynamic coupling. For simplicity, only roots corresponding to the lowest four
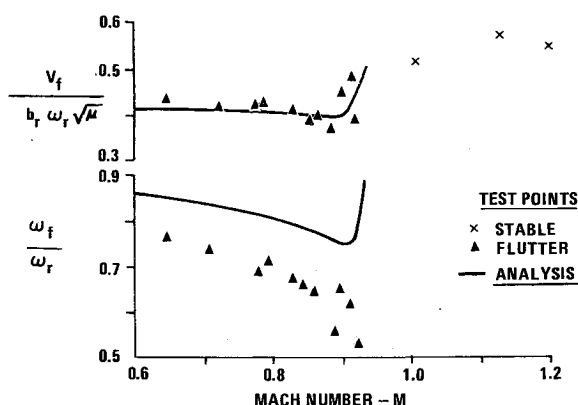
Fig. 6 Experimental and theoretical flutter speed and frequency indices for isolated 100 delta wing.

Fig. 7 Experimental and theoretical flutter speed and frequency indices for isolated 070/040 delta wing.

modes of the system are shown. Without coupling, the basic flutter mechanisms are associated with a coalescence of the first bending and first torsion modes of each surface. In this case, aerodynamic interference lowers the orbiter flutter speed about 10%, while the booster root is raised slightly. Additionally, at a speed 18% lower than the isolated-orbiter flutter speed, an area of marginal instability occurs in which the orbiter bending and booster torsion modes coalesce. An inspection of the eigenvector associated with this instability reveals significant contributions from three modes which are (in order of importance) orbiter torsion, orbiter bending, and booster torsion.

Experimental Flutter Results

Shown in Figs. 6–8 are the flutter speed and flutter frequency indices for the three isolated delta wings. The flutter speed of each has a shallow transonic dip characteristic of delta wings—11%, 10%, and 6% for the 100, 070/040, and 070/032, respectively—while the frequency of flutter is seen to vary considerably with Mach number. A sharp recovery in flutter speed is common to all three wings, and both control-surface models exhibit a buzz region at low supersonic Mach numbers.

Testing of the 100 delta, paired with each of the two 070 deltas, was performed for the separations indicated in Table 2. Two types of interference effects were observed. The first was a simple change in flutter speed on one or both of the surfaces, while the second was a coupled flutter of both surfaces characterized by a common flutter frequency. Films of this mechanism show in one case the surfaces oscillating 180° out of phase; and, upon the flutter destruction of one surface, the other surface can be seen to stabilize.

Flutter boundaries for representative tested interference configurations are shown in Figs. 9–13. In configurations pairing the 070/032 with the 100 delta wing, the subsonic flutter speeds of the flutter critical leading wing are generally reduced. Although no supersonic flutter could be found on the isolated surfaces within wing tunnel bounds,

supersonic flutter occurs on both surfaces for many of these interfering configurations.

For the 070/040 - 100 pairings, the critical subsonic flutter speeds are raised but the leading surface flutters lower than it does without interference. The supersonic recovery is still too high to measure on the leading surface, but that of the 100 wing has been lowered enough to be recorded for several configurations.

In Fig. 14, for each configuration, the ratio of the minimum flutter speed in the transonic dip region to that of the isolated wing is plotted as a function of separation between wing apexes. Only the minimum flutter speed of the flutter critical wing could be determined, since wind tunnel excursions much above the boundary of the flutter critical wing could result in its destruction. Sizable reductions in measured flutter speed of as much as 16% occur for the smaller separations.

Correlation with Analysis

Analyses were run for the configurations denoted in Table 2 over a range of subsonic Mach numbers to produce flutter boundaries. From analyses at a representative tunnel air density, trends of minimum flutter speed as a function of wing separation were determined. Interference typically lowered the flutter speed of the leading wing, while slightly raising that of the trailing wing. Since the flutter critical wing of the 070/032-100 pairing was the leading wing, the minimum flutter speed of that configuration was lowered by interference. Conversely, on the 070/040 - 100 configuration, the trailing wing was critical

Table 2 Configurations[a]

h/c	l/c		
	0.00	0.73	1.45
0.20	A	A&E	A
0.40	A&E	A&E	A
0.60	A&E	A&E	A

[a] A = analysis performed. E = experiment performed.
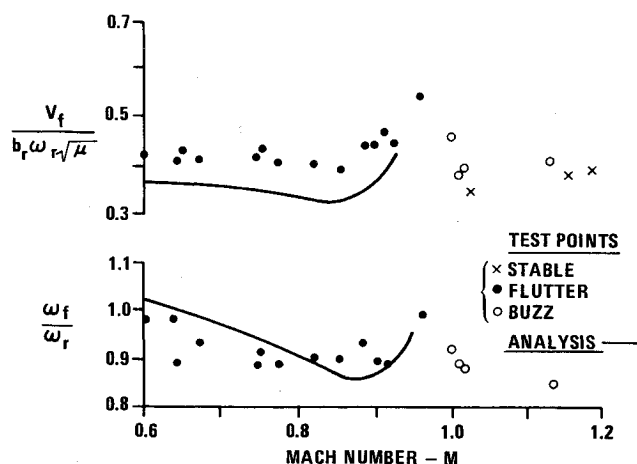
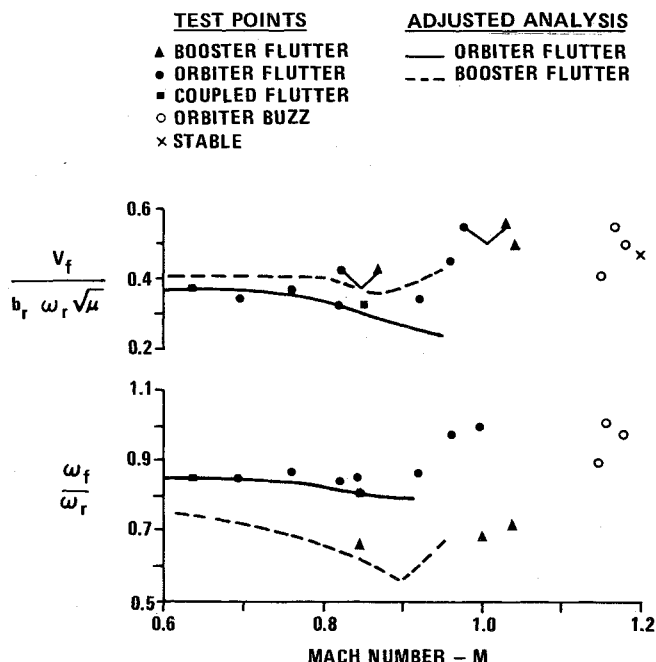Fig. 8 Experimental and theoretical flutter speed and frequency indices for isolated 070/032 delta wing.

Fig. 9 Comparison of experimental and adjusted analytical flutter boundaries for 070/032 and 100 wings, h/c = 0.4, l/c = 0.0.

and interference caused a slight increase in the minimum flutter speed of the pairing. These trends are drawn in Fig. 14 and compare well with test data.

For the 070/032 - 100 configuration the effect of interference diminishes rapidly with streamwise separation; at an apex separation of one mean chord, the flutter-speed reduction is less than 3% for all values or h/c shown. For the 070/040 - 100 configuration, the effect of interference peaks at a nonzero streamwise separation; the flutter-speed is higher for l/c = 0.73 than for l/c = 0.0 or 1.45. The effect of decreasing vertical separation is periodic in streamwise separation: At l/c = 0 or 1.45, the change in flutter-speed increases with decreased vertical separation, while for the intermediate l/c = 0.73, the trend is reversed.

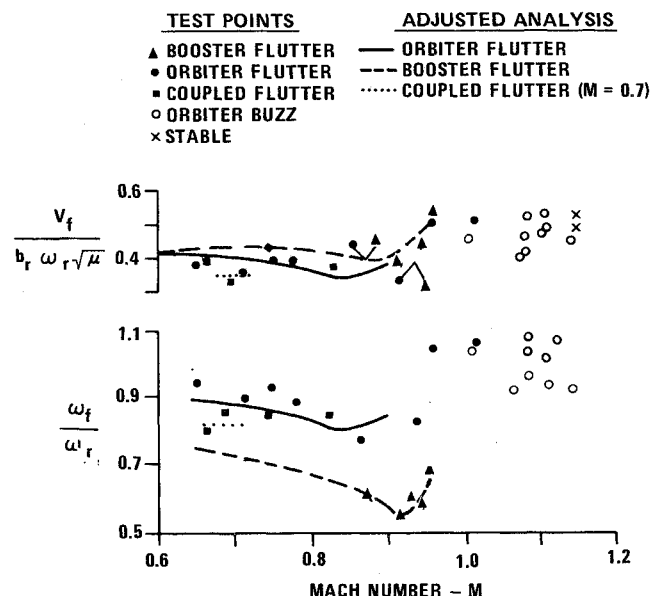To determine the ability of the theory to account for compressibility effects, the analytical flutter boundaries

TEST POINTS   ADJUSTED ANALYSIS
▲ BOOSTER FLUTTER   —— ORBITER FLUTTER
● ORBITER FLUTTER   – – – BOOSTER FLUTTER
■ COUPLED FLUTTER   ······ COUPLED FLUTTER (M = 0.7)
○ ORBITER BUZZ
× STABLE

Fig. 10 Comparison of experimental and adjusted analytical flutter boundaries for 070/032 and 100 wings, h/c = 0.6, l/c = 0.0.
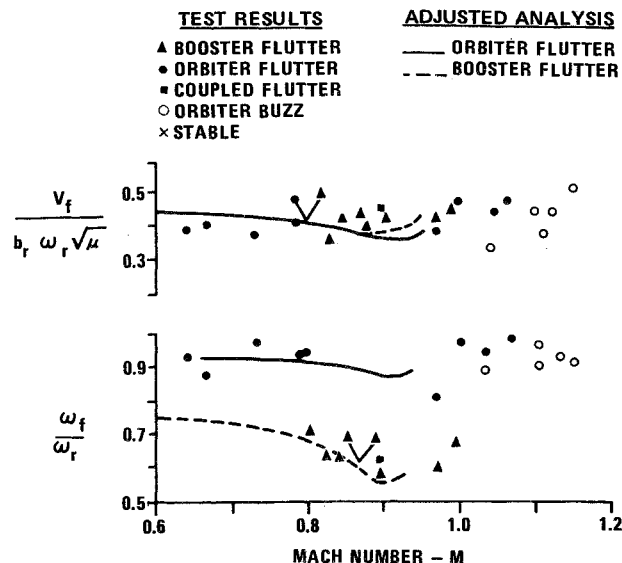
Fig. 11 Comparison of experimental and adjusted analytical flutter boundaries for 070/032 and 100 wings, h/c = 0.4, l/c = 0.73.

were compared with the test boundaries. This correlation was complicated by the nature of the wing tunnel; in a blowdown tunnel the air density is a function of the dynamic pressure and Mach number. Hence, different points on a measured flutter boundary correspond to different air densities, and the effect of compressibility cannot be isolated. To account for differences in air density, the analyses were run for several densities and interpolated to measured tunnel values at various Mach numbers on each boundary.

The analytical boundaries derived by this technique are shown for the isolated wings in Figs. 6–8. Excellent correlation is obtained in the flutter speed of the 100 booster wing: At Mach numbers below the transonic dip, the maximum discrepancy is only 3%. The flutter frequencies predicted for this wing, however, are 12 to 40% larger than measured. On the 070 control surface models, the theoretical flutter speeds are 11 to 19% lower than those occurring in the wind tunnel, while the analytical and test flutter frequencies agree within 5% for the 070/040 and within 12% for the 070/032. The poorer flutter speed prediction on these wings is probably due to the presence of the control surface and the hinge-line gap. On all three wings there are anomalies in the transonic dip prediction. The measured dip is localized to a small band in Mach number while the theory predicts a gradual, less severe trend. Since linearized aerodynamic theory neglects thickness and hence local Mach number effects, it cannot be expected to accurately predict the transonic dip region.

The discrepancies between test and theory found for the isolated wings are, of course, present in the interfering configurations as well. To appraise the theory's ability to predict interference alone, these discrepancies had to be removed. Consequently, the predicted flutter speed and flutter frequency indices of the interfering configurations were adjusted by the ratios of the test-to-analysis indices of the isolated wings. These adjusted indices are presented for five configurations in Figs. 9–13. Except for two areas, the agreement between the flutter speeds of test and analysis is now excellent, indicating that the interference effects have in fact been adequately represented in the analysis.

The first discrepancy is typified by the configuration of Fig. 9 where the analytical orbiter flutter speed does not show the proper recovery. Apparently, the use of isolated surface measured flutter data to correct the theory empirically is not entirely successful at Mach numbers of 0.9
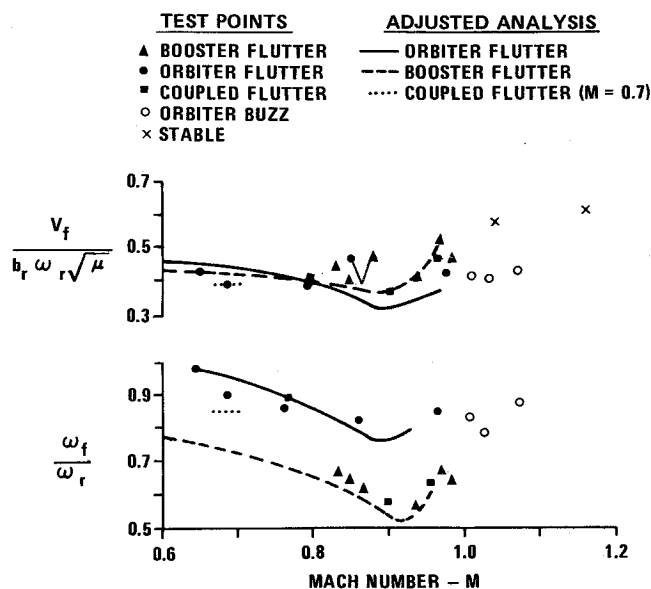
Fig. 12   Comparison of experimental and adjusted analytical flutter boundaries for 070/040 and 100 wings, $h/c = 0.6$, $l/c = 0.0$.

Fig. 13   Comparison of experimental and adjusted analytical flutter boundaries for 070/040 and 100 wings, $h/c = 0.4$, $l/c = 0.73$.

and greater. One reason may be that the venturi effect of the wings in the closer configurations causes the local Mach numbers in the region between them to be significantly different from those of the isolated wings.

The second area of poor agreement exists around $M = 0.7$ on the configuration of Fig. 10, where a coupled instability occurs 15% lower than the predicted level. Strain gage readings taken during testing confirm that sizable motions occur on both surfaces. In further examining the test data that generated this flutter point, it was found that the measured structural dampings of the booster wing used in that tunnel run were much lower than the norm. In fact, the damping of the torsion mode was 50% lower. Referring to Fig. 5, it is seen that the marginal instability neglected thus far in the correlation could be significant for small dampings, and that it lies 11% lower than the next instability. This agrees within $3\frac{1}{2}$% of the measured point. The flutter frequency index calculated for this instability is also reasonable; its value of 0.82 lies between the orbiter and booster flutter frequencies as does the measured value of 0.86. If a similar approach is taken in Fig. 12 at the point near $M = 0.72$, the marginal analytical instability gives a flutter speed index of 0.4, as compared to the test point at 0.41.

To determine the relative importance in aerodynamic interference of wing flexibility as compared to aerodynamic reflections, analyses were rerun for the configuration of Fig. 9 treating the trailing wing as rigid. The reduction in flutter speed due to interference was 11% in this case as opposed to the 16% obtained by test and by analysis with a flexible trailing wing. The flutter frequencies were 11% higher on the average than in the previous analysis. Furthermore, the additional discovered flutter mechanism that couples modes of one wing with those of the other wing are excluded in any such analysis. It can be concluded that treating one wing as rigid and thereby as capable only of reflecting the aerodynamic perturbations of the other wing does not accurately predict the flutter behavior of the coupled pair of wings.

Conclusions

Interference flutter of closely spaced pairs of structurally uncoupled delta wings was studied by experiment and analysis. Significant reductions in the subsonic flutter speed of the leading wings were predicted and observed on
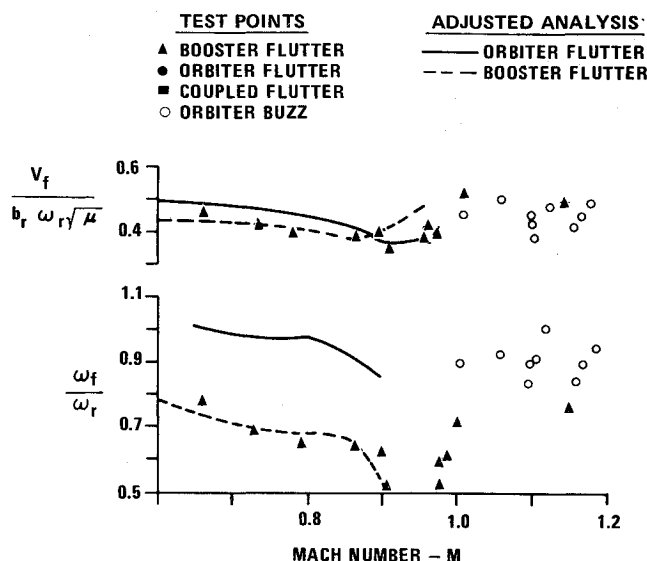
configurations with small wing separations. The subsonic flutter boundary of the large trailing wing was slightly increased by interference. Large reductions in the supersonic flutter boundary of both wings were encountered in testing, indicating the need for analytical methods to investigate this regime.

Except for a difficulty associated with control surfaces, correlation between the flutter speeds of the theory and test in the subsonic range was generally good; the effects of aerodynamic interference were predicted within experimental accuracy.

A new coupled flutter mechanism was predicted and observed in testing models with low structural damping. The instability was characterized analytically by the coupling of the first bending mode of the leading wing with the first torsion mode of the trailing wing and resulted in an 18% lowered flutter speed.
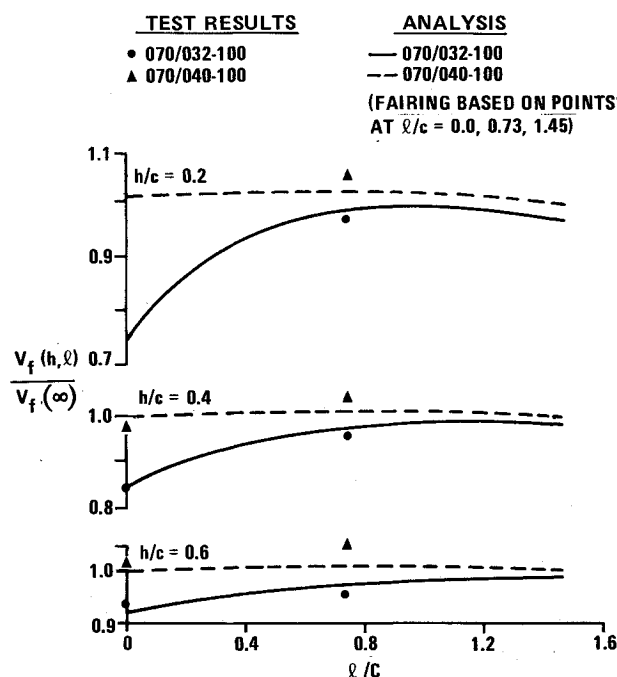

Fig. 14   Effect of wing separation on the minimum transonic flutter speed.

References

[1]Stahle, C. V., "Transonic Effects on T-tail Flutter," RM-24, 1959, The Martin Company, Baltimore, Md.

[2]Stark, V. J. E., "Aerodynamic Forces on a Combination of a Wing and a Fin Oscillating in Subsonic Flow," SAAB TN54, Feb. 1964, Liköping, Sweden.

[3]Laschka, B. and Schmid, H., "Unsteady Aerodynamic Forces on Coplanar Lifting Surfaces in Subsonic Flow (Wing-Horizontal Tail Interference)," AGARD Structures and Materials Panel Meeting, Sept. 25-27, 1967, Ottawa, Canada.

[4]Topp, L. J., Rowe, W. S., and Shattuck, A. W., "Aeroelastic Considerations in the Design of Variable Sweep Airplanes," ICAS Paper 66-12, Sept. 1966, London, England.

[5]Sensberg, O. and Laschka, B., "Flutter Induced by Aerodynamic Interference between Wing and Tail," Journal of Aircraft, Vol. 7, No. 4, July-Aug. 1970, p. 319-324.

[6]Mykytow, W. J., Noll, T. E., Huttsell, L. J., and Shirk, M. H., "Investigations Concerning the Coupling Wing-Fuselage-Tail Flutter Phenomenon," Journal of Aircraft, Vol. 9, No. 1, Jan. 1972, pp. 48-54.

[7]Albano, E. and Rodden, W. P., "A Doublet Lattice Method for Calculating Lift Distributions on Oscillating Surfaces in Subsonic Flow," AIAA Journal, Vol. 7, No. 2, Feb. 1969, pp. 279-285.

[8]Albano, E., Perkinson, F., and Rodden, W. P., "Subsonic Lifting Surface Theory Aerodynamics and Flutter Analysis of Interfering Wing/Horizontal Tail Configurations," AFFDL-TR-70-59, Sept. 1970, Air Force Flight Dynamics Lab., Wright-Patterson Air Force Base, Ohio.

[9]Triplett, W. E., Burkhart, T. H., and Birchfield, E. B., "A Comparison of Methods for the Analysis of Wing-Tail Interaction Flutter," AIAA Paper 70-80, 1970, New York.

[10]Goetz, R. C., "Lifting and Control Surface Flutter," TMX-52876, Vol. III, July 1970, NASA.

[11]Rodden, W. P., Giesing, J. P., and Kalman, T. P., "New Developments and Applications of the Subsonic Doublet-Lattice Method for Nonplanar Configurations," AGARD Symposium, Tönsberg, Oslofjorden, Norway, Nov. 1970.

[12]Chipman, R. R., "Interference Flutter on Space Shuttle Configurations," Paper presented at Aerospace Flutter and Dynamics Council Meeting, May 1972, New York.

[13]Bisplinghoff, R. L. and Ashley, H., Principles of Aeroelasticity, J. Wiley and Sons, New York, 1962.

Aerodynamic Boundary Layer Effects on Flutter and Damping of Plates

E. H. Dowell*

Princeton University, Princeton, N.J.

A previously developed shear flow model for describing the aerodynamic pressures on a moving flexible wall in a boundary layer type flow is utilized to perform stability (flutter) and response analyses for elastic plates. Results for flutter boundaries and damping in the subflutter range are presented and compared to available experimental data. Agreement between theory and experiment is generally good except for damping at low supersonic Mach numbers.

Nomenclature

a, a_∞ = plate length, also speed of sound
b = plate width
D = plate stiffness
E = modulus of elasticity
h = plate thickness
K = $\omega[\rho_m h a^4/D]^{1/2}$
M = U_∞/a_∞, Mach number
q = $\rho_\infty U_\infty^2/2$, dynamic pressure
U = air velocity
z = coordinate perpendicular to plate
λ^* = $2qa^3/D$, nondimensional dynamic pressure
μ = $\rho_\infty a/\rho_m h$, air-to-panel mass ratio
δ = boundary layer thickness
ρ = air density
ρ_m = plate density
ω = frequency
ζ = damping ratio

Subscripts

f = flutter
∞ = freestream

Introduction

IT is now firmly established on experimental grounds that the adjacent fluid shear (boundary) layer can be of importance in modifying the flutter behavior of plates as a result of the recent investigations by Muhlstein, Gaspers and Riddle[1] and Gaspers, Muhlstein and Petroff.[2] The present author has developed a relevant theoretical model which is fully discussed in Ref. 3. Basically the model is an inviscid small perturbation theory with the viscous boundary layer only taken into account through the specification of a nonuniform mean flow. The boundary layer thickness is taken as constant everywhere over the panel. A more complete analysis would include viscous effects in the perturbations as well, i.e., one would employ a dynamic linearization of the Navier-Stokes equations about the same mean flow. Whether this latter model is needed for some applications is still an open question. However the simpler theory of Ref. 3 has already proven useful, and here we explore its potentiality further. Specifically we make comparisons with experimental flutter data over a larger parameter range than that considered in Ref. 3 and also make initial comparisons with experimental data for the aerodynamic damping for conditions below the flutter boundary. By aerodynamic damping we mean the damping provided to the plate by the aerodynamic flow. The structural model is a rectangular isotropic plate clamped on all edges. This paper is a continuation of Ref. 3 where the interested reader may find the mathematical details of the analysis.